Journal of
Materials Chemistry C

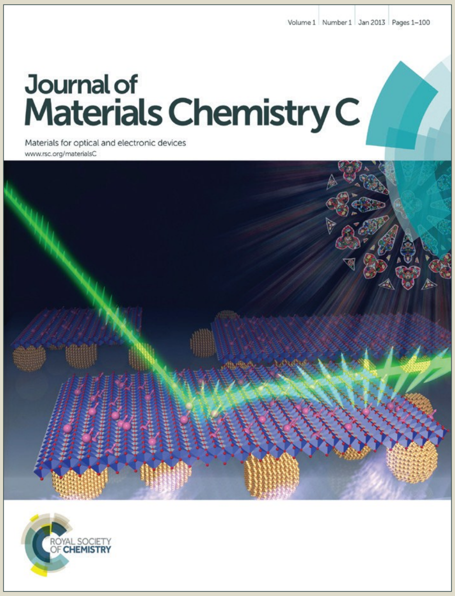

ROYAL SOCIETY
OF CHEMISTRY

www.rsc.org/materialsC

Journal Name

Journal of Materials Chemistry C

Dynamic Article Links ►

Cite this: DOI: 10.1039/c0xx00000x

www.rsc.org/xxxxxx

ARTICLE TYPE

White OLEDs Based on a Novel Eu^{III}–Tetrakis–β–Diketonate Doped into 4,4'-*N*,*N*'-Dicarbazolebiphenyl as Emitting Material†

Silvanose Biju, Liang-Jin Xu, Cheng-Zhe Sun and Zhong-Ning Chen*

Received (in XXX, XXX) Xth XXXXXXXXX 20XX, Accepted Xth XXXXXXXXX 20XX

DOI: 10.1039/b000000x

Color tunable electroluminescence is obtained from devices having spin-coated single emitting layer with a novel Eu^{III}–tetrakis–β-diketonate complex $NBu_4[EuL_4]$ (L^- = 4-(4'-Carbazol-9-yl-biphenyl-4-yl)-1,1,1-trifluoro-4-oxo-but-2-en-2-ol anion) doped to CBP (4,4'-*N*,*N*'-dicarbazolebiphenyl)-OXD7 (1,3-bis[2-(4-tert-butylphenyl)-1,3,4-oxadiazo-5-yl]benzene) blend. The external quantum efficiency (EQE) as high as 2.8%, maximum brightness (L) of 1547 cd m^{-2}, current efficiency (η_c) of 5.14 cd A^{-1} and power efficiency (η_p) of 2.53 lmW^{-1} were shown by a device having the structure ITO / PEDPT:PSS(50 nm) / CBP (56%) : OXD7 (24%) : $NBu_4[EuL_4]$ (20%) (50 nm) / TPBI (50 nm) / LiF (1.5 nm) / Al (120 nm). The newly designed β-diketonate ligand containing hole-transporting carbazole group and π-spacer extends the excitation window of the Eu^{III}-complex to 450 nm and also improves the carrier transport properties. The modification in the ligands results in low turn-on voltage of the devices (<5V). Furthermore, the devices containing 10-20% $NBu_4[EuL_4]$ in the emitting layers show white emission in wide voltage range (8–13V) with sizable efficiencies.

Introduction

The white organic light emitting diodes (WOLEDs), which can be considered as high performance alternatives for the existing low efficient incandescent and fluorescent lights, have become a major area of research interest in recent years.[1] Even though a very large number of white organic electroluminescent devices using organic dyes, polymers and organometallic complexes have been extensively reported,[1] organo-lanthanide (Ln^{III}) complexes are still of great interest because of unique ability to emit ion specific, narrow line-like emission bands in the visible region.[2-4] In principle, white emission requires the mixing of three primary colours (blue, green, and red) or two complementary colours (blue and yellow or orange). Kido et al. obtained while light from a multilayered device consisting of Eu^{III} (red) and Tb^{III} (green)-complexes in the emitting layer.[5] Later Zhao et al. developed a binuclear complex $Eu_xTb_{1-x}(acac)_3phen$ which can emit both red and green colours simultaneously and produced white light in combination with the blue light from the TPD/NPB host.[6] In a similar work Quirino et al. realized white electroluminescence from unsymmetrical binuclear complex involving $Eu(BTFA)_3$ and $Tb(acac)_3$ connected through a bidentate terpyridine ligand.[7] Near white electroluminescence (CIE, x = 0.33, y = 0.38) was achieved from solution processed OLED containing Eu^{III}- and Tb^{III}- tetrakis-β-diketonates in two different emitting layers.[8] However, the efficiencies of the above mentioned devices were not satisfactory. Moreover, these devices with additional emitting layer will make the device fabrication more complex and expensive. The best solutions for this problem is to use a single-component emitter with tunable energy transfer process, which can have the additional advantages such as higher stability, better reproducibility, no phase separation, and low production costs.[9-11] In this context, WOLEDs containing mononuclear Eu^{III}-complexes doped in a conducting polymer which can emit blue-green lights are well investigated.[12,13] In another unique example, Law et al. showed that white light can be generated from OLEDs containing single molecular Eu^{III}-complex which can emit blue, green and red emissions simultaneously.[14] However it required a relatively higher voltage of 16 V to achieve white light (CIE, x = 0.34, y = 0.35).

Fluorinated-β-diketonates with organic chromophores have a ubiquitous role in lanthanide coordination chemistry because they can chelate and sensitize Eu^{III} ion simultaneously.[15-17] Unfortunately, their poor carrier-transport ability cannot satisfy the need of fabricating OLEDs and limits their practical applications.[4,18,19] The carrier-transport properties of lanthanide complexes can be improved by introducing the charge-transport groups to the chelating ligands.[20] Carbazole exhibits many advantages to the application because of inexpensive starting material, good chemical and environmental stability, and being easily anchored with a wide variety of functional groups to tune the optical and electrical properties.[21,22] Because of these reasons, numerous Eu^{III}-β-diketones containing carbazole moieties have been reported.[23-25] In most cases, the β-diketone moiety is attached to the 3-, 6- or 2-, 7- positions of the carbazole ring. For instance, He et al. obtained blue-light excitable Eu^{III}-β-diketonates containing 2,7-position substituted carbazole ring.[26]

However, the photoluminescent efficiency was not satisfied for OLED technology requirements due to the back energy transfer from Eu^{III} to the ligand states. N-substituted carbazole units are well known for their efficient photoconduction and charge-transporting properties and hence they were introduced widely to numerous host materials used in the emitting layers of OLEDs such as poly(N-vinylcarbazole) (PVK), 1,3-bis(9-carbazolyl)benzene (mCP), 4,4',4"-tri-(N-carbazolyl)triphenylamine (TCTA) and 4,4'-N,N'-dicarbazole-biphenyl (CBP) etc. Li et al. obtained white light emission (CIE, x = 0.333, y = 0.348) with external quantum efficiency 1.1% and maximum brightness of 229 cd m^{-2} from a device having the structure ITO / NPB / CBP : $Eu(TCPD)_3(Phen)$ / BCP / Mg : Ag, where $Eu(TCPD)_3(Phen)$ is (tris[1-[3,4,5-tris[4-(9H-carbazol-9-yl)butoxy]-phenyl]-3-phenylpropane-1,3-dione])(1,10-phenanthroline)europium(III), a dendritic Eu^{III} complex containing carbazole units grafted through the N-atom.[27]

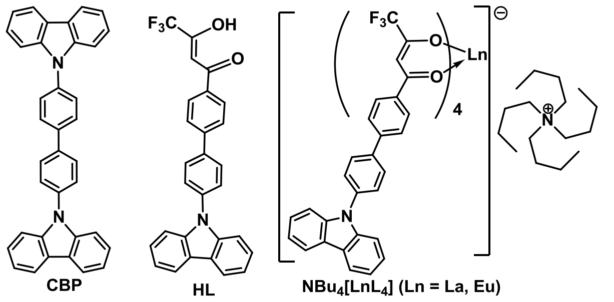

Fig. 1 Chemical structures of the host CBP, the ligand HL and its Ln^{III} complexes.

Inspired from the above mentioned reports, in the present study we have synthesized a new fluorinated β-diketone containing N-biphenyl carbazole chromophore (HL). The synthesized ligand is complexed with Ln^{III} ions (Ln= Eu, La) in tetrakis manner. Tetrakis-*β*-diketonate complexes of Ln^{III} are known to be promising, due to their high thermal and chemical stabilities, larger cross section of photon absorption and charge carrier trapping and higher luminescence quantum yields than the widely studied tris complexes.[18] Moreover, due to the structural similarities of HL (Fig. 1) with that of host CBP, good energy level matches and phase compatibility for $NBu_4[EuL_4]$ with the host is expected. This can prevent crystallization of $NBu_4[EuL_4]$ and may increase the electroluminescence efficiencies and lifetime of the devices.

Experimental

Materials. Lanthanide(III) nitrate hexahydrates 99.99% (Ln = Eu, La) were obtained from Sigma Aldrich. 4-(9H-Carbazol-9-yl)phenylboronicacid 98 % (Sukailu), 4-bromo-acetophenone 98% (Beijing HWRK Chem), ethylTrifluoroacetate 98% (Accela Chem Bio) and tetra-*n*-butylammoniumbromide 98% (Acros Organics) were used without further purification. Solvents were dried using standard methods. All the other chemicals used were of analytical reagent grade.

Methods. Infrared spectra (IR) were recorded on a Magna 750 FT-IR spectrophotometer with KBr (neat) pellets. Elemental analysis (C, H, N) was carried out on a Perkin-Elmer model 240 C elemental analyzer. Electrospray ionization mass spectrometry (ESI-MS) was performed on a Finnigan LCQ mass spectrometer and HRMS on Synapt G2b Waters using dichloromethane as mobile phases. ^1H and ^{13}C NMR spectra were recorded on a Bruker Avance III 400 spectrometer with $SiMe_4$ as internal reference. The thermogravimetric analysis (TGA) was performed on a TGA-50H instrument (Shimadzu, Japan). The cyclic voltammogram (CV) was measured using a potentiostat/galvanostat model 263A in dichloromethane solution containing 0.1 M $(Bu_4N)(PF_6)$ as the supporting electrolyte. CV was performed at a scan rate of 100 mV s^{-1} and DPV at a rate of 20 mV s^{-1} with a pulse height of 40 mV. Platinum and glassy graphite were used as the counter and working electrodes, respectively, and the potential was measured against Ag/AgCl reference electrode. UV−vis absorption spectra were measured on a Perkin-Elmer Lambda 35 UV−vis spectrophotometer. Photoluminescence emission, excitation, excited state lifetimes (solid state) and electroluminescence emission spectra were recorded on an Edinburgh analytical instrument (FLS920 fluorescence spectrometer). The PL emission quantum yields ($\phi_{overall}$) in solid-state were determined by the absolute method using an integrating sphere attached to FLS920 fluorescence spectrometer. All the spectra were corrected for experimental responses.

Device Fabrication and Characterization: The devices were fabricated on indium tin oxide (ITO) coated glass substrates. Patterned ITO coated glass substrates were washed with acetone, detergent, distilled water and isopropanol, subsequently in an ultrasonic bath. After UV Ozone treatment for 15 minutes, PEDOT: PSS (Batron-P 4083, Bayer AG) from water solution was spin-coated (at 3000 rpm) onto the substrate followed by drying in a vacuum oven at 140 ℃ for 20 min, giving a film of 50 nm thickness. A mixture of CBP/OXD7 and $NBu_4[EuL_4]$ in CH_2Cl_2 (5.5 mg/mL) was spin-coated on the top of PEDOT: PSS (at 1500 rpm). Typically, the thickness of the emitting layer was around 50 nm. The TPBI layer (50 nm) was then thermally deposited followed by a thin layer of LiF (1.5 nm) with a 120 nm thick Al capping layer deposited through a shadow mask in a chamber with a base pressure of around 10^{-4} Pa. Current density (*J*)-voltage (*V*)-luminance (*L*) data was collected using a Keithley 2400/2000 source measurement unit and a calibrated silicon photodiode. The brightness in cd m^{-2} was measured by a silicon photodiode.

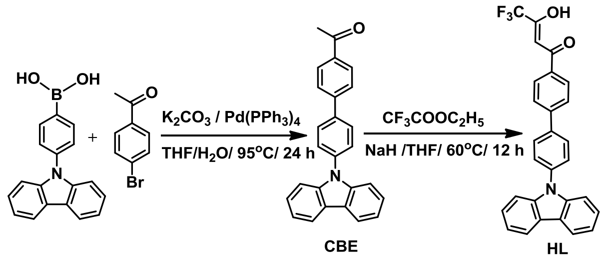

Scheme 1. Synthetic procedure for ligand HL.

Synthesis of ligand HL. The ligand HL was prepared in two steps with an overall yield of 60% (Scheme 1). In the first step, a mixture of 4-(9H-carbazol-9-yl) phenylboronicacid (10 mmol), 4-bromoacetophenone (11 mmol) and catalytic quantity of $Pd(PPh_3)_4$ in degassed aqueous K_2CO_3 (20%)/THF (1:1, v:v) (60 mL) was stirred and heated at 95 ℃ for 1 d under inert atmosphere. The hot mixture was cooled and the precipitate was filtered to get a pale yellow solid. This solid was insoluble in common organic solvents and hence purified by washing with CH_2Cl_2 (3 × 50 mL) to remove the unreacted starting materials. Thus obtained 1-(4-(9H-carbazol-9-yl)biphenyl) ethanone (CBE) in 60% yield was used for the next step without further purification. Yield: 60%. Anal. Calcd for $C_{26}H_{19}NO$ (361.44): C, 86.40; H, 5.30; N, 3.88; Found: C, 86.65; H, 5.51; N, 4.00%.

In the second step, to the dispersion of 1-(4-(9H-carbazol-9-yl)biphenyl)ethanone (CBE) synthesized in the first step (10 mmol) in 50 mL of dry THF, NaH (11 mmol) was added and stirred for 10 min at 0 ℃. To this solution, ethyltrifluoroacetate (11 mmol) was added dropwise in an inert atmosphere and the temperature was increased to 60 ℃ with stirring for another 12 h. To the resulting yellow solution, 50 mL of 2 M HCl was added, and the mixture was extracted with dichloromethane (2 × 50 mL). The organic layer was separated and dried over $MgSO_4$, and the product was obtained as fine yellow crystals on keeping its concentrated CH_2Cl_2 solution for one day. Yield: 60%. Anal. Calcd for $C_{28}H_{18}F_3NO_2$ (457.44): C, 73.52; H, 3.97; N, 3.06. Found: C, 73.97; H, 4.11; N, 3.21%. FTIR (KBr, cm^{-1}): 3450 (ν_s O–H); 3042, (ν $C_{sp2}H$); 1599 (ν_s C=O); 1526, 1495, 1461, 1450 (ν C=C); 1364, 1318, 1286 (ν_sC–N); 1147, 1098 (δC–H); 1107 (ν_sC–F); 841, 790 (δ C–H), 716 (δ CF_3). ^1H NMR ($CDCl_3$, 400 MHz), δ (ppm): 6.68 (1H, s), 7.33-7.37 (2H, t; J = 7.4 Hz), 7.45-7.53 (4H, m; J = 7.9 Hz), 7.72-7.74 (2H, d; J = 8.0 Hz), 7.84-7.91 (4H, q; J = 8.3 Hz), 8.10-8.12 (2H, d; J = 8.0 Hz), 8.19-8.29 (2H, d; J = 7.6 Hz), 15.23 (1H, s: broad). ^{13}C NMR ($CDCl_3$, 400 MHz) δ (ppm): 92.32 (CO–CH–CO); 109.75-145.80 (carbazole/biphenyl); 131.87 (CF_3); 177.65, 185.46 (CO). ESI-MS: m/z = 456.6 (100%) $[M–H]^-$.

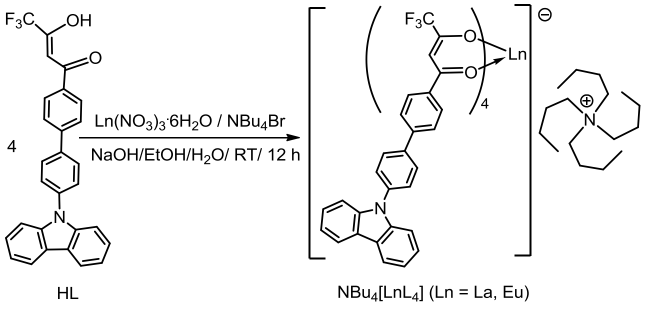

Scheme 2. Synthetic procedure for Ln^{III} complexes $NBu_4[LnL_4]$ (Ln = La, Eu).

Synthesis of Ln^{III} complexes NBu_4 $[LnL_4]$. To an ethanolic suspension of HL (1 mmol) was added 1 mL of aqueous NaOH (1 M) at room temperature and the mixture was stirred until complete dissolution of HL. Required volumes of aqueous Ln^{III} nitrates were then added slowly and the solution was diluted to 50 mL. The reaction mixture was then stirred for 6 h at room temperature. A solution of Bu_4NBr (1.05 mmol) in deionized water/ethanol (5/10 mL) was then added, resulting in the formation of a precipitate (Scheme 2). After further stirring the mixture for 6 h at room temperature, pale yellow solid product was filtered, washed with cold ethanol, and dried. The obtained $NBu_4[LnL_4]$ complexes were re-dissolved in CH_2Cl_2, and were allowed to stand for a period of 1–2 weeks. The $NBu_4[LnL_4]$ complexes were obtained as amorphous powder. The products were dried in vacuum at 50 ℃ for 1 day.

$NBu_4[LaL_4]$ (yellow solid). Yield: 94%. Elemental analysis (%) calcd. for $C_{128}H_{104}LaF_{12}N_5O_8$ (2207.11): C, 69.66; H, 4.75; N, 3.17. Found: C, 69.92; H, 4.88; N, 3.45%. FTIR (KBr, cm^{-1}): 3050 (ν $C_{sp2}H$); 2977, 2955, 2923, 2852 (ν $C_{sp3}H$); 1626, 1602 (ν_s C=O); 1531, 1496, 1460, 1451 (ν C=C); 1362, 1318, 1286 (ν_sC–N); 1147, 1097 (δC–H); 1105 (ν_sC–F); 841, 791 (δ C–H), 715 (δ CF_3). ^1H NMR ($CDCl_3$, 400 MHz), δ (ppm): 1.01-1.04 (12H, m; J = 4.0 Hz) 1.409-1.476 (8H, m; J = 4.0 Hz), 1.51-1.73 (8H; J = 4.0 Hz), 3.01-3.40 (8H; J = 4.0 Hz), 6.53 (4H, s), 7.31-7.47 (24H, m; J = 7.0 Hz), 7.48-7.83 (24H, m; J = 8.0 Hz), 8.16-8.18 (16H, m; J = 8.0 Hz). ESI-MS: m/z = 1964.4030 (40%) $[(LaL_4)]^-$.

$NBu_4[EuL_4]$ (yellow solid). Yield: 95%. Elemental analysis (%) calcd. for $C_{128}H_{104}EuF_{12}N_5O_8$ (2220.17): C, 69.25; H, 4.72; N, 3.15. Found: C, 69.71; H, 4.94; N, 3.54%. FTIR (KBr) ν_{max} (cm^{-1}): 3053 (ν $C_{sp2}H$); 2975, 2959, 2936, 2873 (ν $C_{sp3}H$); 1627, 1601 (ν_s C=O); 1528, 1495, 1461, 1450 (ν C=C); 1363, 1318, 1286 (ν_sC–N); 1147, 1098 (δC–H); 1106 (ν_sC–F); 842, 791 (δ C–H), 716 (δ CF_3). ESI-MS: m/z = 1977.4169 (40%) $[(EuL_4)]^-$.

Results and Discussion

Spectroscopic Characterization of Ln^{III}-Complexes

The ligand **HL** was prepared by the well-known Suzuki coupling followed by Claisan condensation with an overall yield of 60% (Scheme 1). The ^1H and ^{13}C NMR spectra of HL (Figs. S1 and S2 in ESI†) show that the ligand exists as enol form in solution. The synthetic procedures employed for $NBu_4[LnL_4]$, (Ln=La, Eu) are described in Scheme 2. FT-IR, ^1H NMR spectroscopy (Fig. S3 in ESI†). and microanalysis data for Ln^{III} complexes $NBu_4[LnL_4]$, (Ln=La, Eu) demonstrate that the Ln^{III} : L^- mole ratio is 1 : 4 and that one molecule of counter cation (NBu_4^+) is present. The carbonyl stretching frequency ν_s(C=O) of HL (1599 cm^{-1}) shifts to 1626-1627 cm^{-1} in $NBu_4[LnL_4]$, (Ln=La, Eu) along with the appearance of a new peak in the range 1601-1602 cm^{-1}, thus indicating coordination of carboxylates to the Ln^{III} cation in each case. Furthermore, the presence of signals in the range 2800 – 3000 cm^{-1} due to the $–CH_2–$ groups and the signal around 1200-1300 cm^{-1}, ν_s(C–N), confirm the presence of NBu_4^+ in the complexes. The absence of any broad bands around 3500 cm^{-1} ν_s(O–H) in $NBu_4[LnL_4]$, (Ln=La, Eu) proves that they are anhydrous and, therefore, that all four β-diketonate ligands are coordinated to the Ln^{III} cations. The high resolution ESI mass spectral analysis (Figs. S4 and S5 in ESI†) of $NBu_4[LnL_4]$ samples (Ln = La, Eu) shows peaks at m/z = 1964.4030 (40%) $[(LaL_4)]^-$and 1977.4169 (40%) $[(EuL_4)]^-$, confirming that these complexes are tetrakis in nature. The thermal stability of the Ln^{III}-complexes in air was examined by thermogravimetric analysis and typical thermograms are depicted in Fig. S6 (ESI†). From the Fig. S6, it is evident that the decomposition temperature (T_d) of $NBu_4[LnL_4]$ are 200 °C. These T_d value is falling in the range expected for Ln^{III}-complexes without solvent molecules in the first coordination sphere. Further thermal decomposition of $NBu_4[LnL_4]$ appears with steps around 225-300, 300-400 and 400-650°C, corresponding to the loss of organic groups and formation of the Lanthanide oxides. The residual weights (7.6 – 8.2%) correspond to the weight of rare-earth oxides (calcd. 7.4 – 7.9 %).

Electronic Spectroscopy and Ligand-Centred Energy Levels

The UV-Vis absorption spectra of the new ligand HL and its Ln^{III}-complexes in CH_2Cl_2 solutions were recorded at room temperature and are presented in Fig. 2. Relevant data are gathered in Table 1. The absorption profile of free ligand HL show a maximum at 240 nm due to the $^1(\pi-\pi^*)$ absorption of the carbazole moiety[28] and a less intense absorption band in low energy region (342 nm), which can be attributed to the $^1(\pi-\pi^*)$ enol absorption of aromatic β-diketone.[29,30] The lower energy absorption band of ligand HL is red-shifted by 13 nm compared to the one reported for the HBTFA (λ_{max} = 329 nm in DMF),[30] probably due to the elaboration of conjugation length. The absorption spectra of Ln^{III} complexes are similar to that of free ligand. This is in accordance with the fact that the coordination of Ln^{III} ions with β-diketonate moieties has little effect on coordination. Furthermore, the molar absorption coefficients of the lowest-energy transition for $NBu_4[LnL_4]$ (100400–101150 M^{-1} cm^{-1}) are approximately four times higher than the value for the free ligand (27080 M^{-1} cm^{-1}), pointing to the presence of four L^- anions bonded to each Ln^{III} cation. The energy of the singlet state level of the ligand was calculated from the higher wavelength absorption edge of the absorption spectrum of $NBu_4[LaL_4]$, and is equal to 25200 cm^{-1} / 3.12 eV (397 nm).

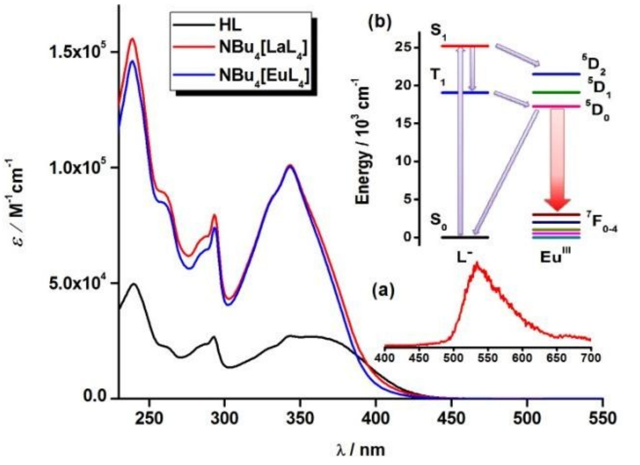

Fig. 2 UV-Vis absorption spectra of HL and its Ln^{III}-complexes in CH_2Cl_2 at 298 K; (c ~ 1×10^{-5}): inserts; (a) Corrected phosphorescence spectra of $NBu_4[LaL_4]$ at 77 K in $CDCl_3$, (c ~ 1×10^{-5}, delay increment 0.5 ms, λ_{ex} = 343 nm); vertical scales are arbitrary units, (b) energy transfer diagram of $NBu_4[EuL_4]$.

The ligand-centred absorption bands in Eu^{III} complexes can undergo intersystem crossing leading to enhanced population of its lowest triplet level and subsequent energy transfer to the nearby ^5D_J states.[31] This mechanism will not work for the La^{III} complexes due to the lack of 4*f*-electrons. Thus the investigation of the phosphorescence spectra of the $NBu_4[LaL_4]$ complex at low temperature gives useful information about the ligands triplet state. Fig. 1, insert (a) displays the phosphorescence spectrum of $NBu_4[LaL_4]$ at 77 K obtained by excitation at 342 nm. The emission band centred around 540 nm can be considered as the emission from the triplet $(^3\pi-\pi^*)$ state of bound L^-. The energy of the lowest triplet states was calculated from the higher wavelength emission edge and the value is 19050 cm^{-1} / 2.36 eV (525 nm). The $^1(\pi-\pi^*)$ and $^3(\pi-\pi^*)$ state energies of L^- are higher than receiving Eu^{III} ($^5D_{0-2}$) states and hence efficient sensitization can be expected. However, ΔE = $^3(\pi-\pi^*)$ – $^5D_0$ = 1800 cm^{-1} is not sufficient enough to prevent the back energy transfer.[32] A schematic energy level diagram and energy transfer processes in $NBu_4[EuL_4]$ are sketched in Fig.1, insert (b).

Table 1. UV-Vis absorption spectral data of the ligand HL and its Ln^{III}-complexes in CH_2Cl_2 at 298 K; (c ~ 1×10^{-5}).

Compound	λ_{max} / nm (ε / M^{-1} cm^{-1})	
HL	342 (27078)	240 (49614)
$NBu_4[LaL_4]$	343 (101152)	239 (155657)
$NBu_4[EuL_4]$	343 (100412)	239 (146004)

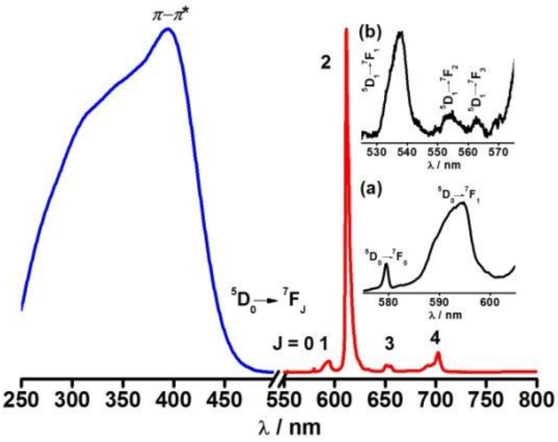

Fig. 3 Corrected, normalized excitation (λ_{em}= 612 nm) and emission (λ_{ex}= 400 nm) spectra of $NBu_4[EuL_4]$,at 298K in solid state; vertical scales are arbitrary units; inserts (a) enlarged view of $^5D_0 \rightarrow ^7F_{0\text{-}1}$ transitions, (b) enlarged view of $^5D_1 \rightarrow ^7F_{1\text{-}3}$ transitions.

Eu^{III}-Centred Photoluminescence Properties

The room temperature PL excitation and emission spectra of $NBu_4[EuL_4]$ recorded in solid state are depicted in Fig.3. The excitation spectrum composed of a broad band covering the entire UV region and extended up to visible region (250-450 nm) with a maximum around 400 nm and a high energy shoulder at 300 nm. The maximum around 400 nm can be attributed to the $^1(\pi-\pi^*)$ absorption of the aromatic β-diketonate, whereas the higher energetic shoulder is due to the $^1(\pi-\pi^*)$ absorption of the carbazole group. The Eu^{III}-centred excitation lines due to $^7F_0 \rightarrow$ $^5F_4$ (296 nm), $^5H_6$ (362 nm), $^5D_4$ (381 nm), $^5G_4$ (394 nm), $^5L_6$ (415 nm), $^5D_3$ (466 nm), $^5D_2$ (527 nm) and $^7F_1 \rightarrow$ $^5D_1$ (533 nm) transitions were hardly observed as they are overlapped by the broad ligand centred bands which can be regarded as a strong evidence in favour of antenna mechanism.[33-36] The emission spectrum of $NBu_4[EuL_4]$ recorded in solid state by exciting at the excitation maximum (400 nm) comprises the characteristic emissions lines at 582, 593, 612, 653 and 702 nm, which originate from Eu^{III} ion corresponding to $^5D_0 \rightarrow 7F_J$ (J = 0–4) radiative deactivation transitions.[33-36] The lack of the broadening emission bands arising from the ligands suggests the efficient intramolecular energy transfer from the carbazole and β-diketonate moieties of the ligand (L^-) to Eu^{III} ion. The spectrum is dominated (85%) by the so-called hypersensitive $^5D_0 \rightarrow {}^7F_2$ transition, which is responsible for the highly intense red luminescence with CIE coordinates x = 0.610, y = 0.315. The intensity ratio, $R = (I_{5D0\rightarrow7F2} / I_{5D0\rightarrow7F1})$ was found to be 17.4, a typical value expected for Eu^{III}-tetrakis-β-diketonates. Such a high R value was only possible when the Eu^{III} ion did not occupy a site having inversion symmetry.[33-36] Thus it is clear that strong coordination interactions took place between the β-diketonate anion and Eu^{III} cation in $NBu_4[EuL_4]$. Furthermore, the emission spectrum of the complex showed only one signal for the $^5D_0 \rightarrow {}^7F_0$ transition (Fig. 3; insert a), indicating the presence of a single chemical environment around the Eu^{III} ions.[30,33,36] Apart from these highly intense emission lines, the emission spectrum of $NBu_4[EuL_4]$ shows some faint signals in the higher energy region (Fig. 3, insert b) due to the transitions $^5D_1 \rightarrow {}^7F_J$ (J =1-3). The presence of such signals is pointing towards the possibility of a less common energy transfer process involving the $^1(\pi-\pi^*)$ state of ligand and higher excited states ($^5D_{1-3}$) of Eu^{III} [37] (Fig. 1, insert a).

The $^5D_0$ lifetime (τ_{obs}) of $NBu_4[EuL_4]$ was investigated by exciting the sample at 400 nm and monitoring the intense $^5D_0 \rightarrow {}^7F_2$ transition at 612 nm at 298 K. The decay curve could be fitted with single exponential function ($\tau_{obs} = 469 \pm 5 \mu s$), consistent with the presence of a single major luminescent species in the complex (Fig. S7 in ESI†). The radiative lifetime (τ_{rad}) and the Eu-centred luminescence quantum yield (intrinsic quantum yield; ϕ_{Eu}) are evaluated by the equations $1/\tau_{rad} = A_{MD,0} \times n^3 \times (I_{tot}/I_{MD})$ and $\phi_{Eu} = \tau_{obs} / \tau_{rad}$,[30,34,38] where $A_{MD,0}$ = 14.65 s^{-1} is the spontaneous emission probability for the $^5D_0 \rightarrow {}^7F_1$ transition *in vacuo*,[17,30] n = 1.5[30,33] is the refractive index, I_{tot}/I_{MD}= 20.4 is the ratio of the total area of the corrected Eu^{III} based emission spectra to the area of the magnetic-dipole allowed $^5D_0 \rightarrow {}^7F_1$ transitions. The overall quantum yield of Eu^{III} sensitized emission ($\phi_{overall}$), which is the ratio between the number of photons absorbed by the antenna to the number of photons emitted by the Eu^{III} ion is regulated by the sensitization efficiency of the antenna molecule (ϕ_{sen}), and the intrinsic luminescence quantum yield of the Eu^{III} ion (ϕ_{Eu}): $\phi_{overall} = \phi_{sen} \times \phi_{Eu}$.[30,33,36] The $\phi_{overall}$ for $NBu_4[EuL_4]$ was determined at room temperature by an absolute method. The parameters obtained for $NBu_4[EuL_4]$ in solid state at 298 K are radiative lifetime (τ_{rad}) of 995 s^{-1}, intrinsic quantum yield (ϕ_{Ln}) of 47%, sensitization efficiency (ϕ_{sen}) of 96 %, and overall quantum yield ($\phi_{overall}$) of 45 ± 5 %.

Electroluminescence performance and chromaticity of OLEDs

A series of EL devices with configuration ITO / PEDOT : PSS (50 nm) / CBP : OXD7 (7 : 3) : $NBu_4[EuL_4]$ (10-100%) (50 nm) / TPBI (50 nm) / LiF (1.5 nm) / Al (120 nm) were fabricated and investigated. Here the emitting layer is $NBu_4[EuL_4]$ with a doping concentration of 10-100 wt% in CBP (70%) and OXD7 (30%) blend. CBP is an excellent host for phosphorescent dopants due to its high triplet energy of 2.56 eV and ambipolar charge-transporting ability.[39] The presence of OXD7, which is a good electron-transport host, will balance the electron and hole carriers within the emitting layer. The energy values of HOMO and LUMO of $NBu_4[EuL_4]$ were estimated from the result of cyclic voltammetry (Fig. S8 in ESI†) and absorption spectrum. From the Fig. 4, it can be seen that the HOMO level of $NBu_4[EuL_4]$ fall within that of the CBP host with a shallow hole trap depth of 0.08 eV and at the same time its LUMO value (2.7 eV) is same as that of the electron transport layer TPBI. This peculiar alignment of energy levels may facilitate efficient charge trapping and recombination within the emitting layer.

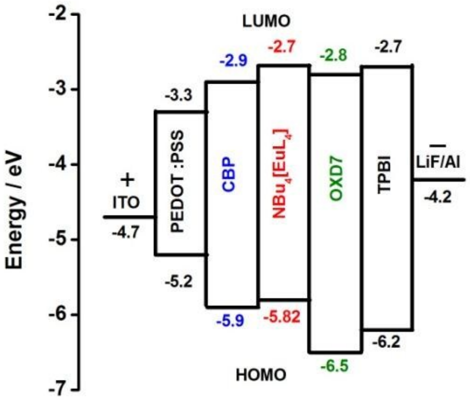

Fig. 4 Energy level diagram of the devices.

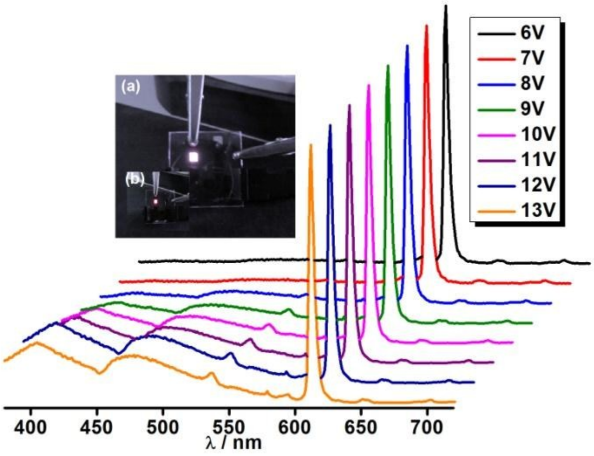

Fig. 5 Electroluminescence spectra of $NBu_4[EuL_4]$ based on device configuration ITO / PEDOT: PSS (50 nm) / $NBu_4[EuL_4]$ (10%) : CBP(63%) - OXD7 (27%) (50 nm) / TPBI (50 nm) / LiF (1.5 nm) / Al (120 nm) at different bias voltages: inserts photograph of device at 9 V (a) and 7 V (b).

The EL spectra of the devices at 10wt% and 20wt% doping concentration show only the characteristic sharp red Eu^{III}-emission peak at 612 nm ($^5D_0 \rightarrow {}^7F_2$), the intensity of which increases with applied voltage up to 7 V (Figs. 5 and 6). With further increase in voltage, the EL spectra of both the devices (Figs. 5 and 6) show two broad bands in the higher energy regions. The first band with maxima around 400 nm is due to the blue emission from the host CBP and the second band with maxima around 480 nm can be attributed to the emission of exciplexes and/or excimers from CPB : $[EuL_4]^-$. The contribution from $^5D_1\rightarrow{}^7F_1$ transition of Eu^{III} at 536 nm towards green light cannot be ignored. Thus the blue emission from CBP combined with the green emission from exciplex and/or eximer and Eu^{III}-centred red emission results in white emission (Fig. 7) in wide range of voltages (8–13V) (Table S1 in ESI†). Nearly perfect white luminescence was achieved at 9 V (x = 0.337, y = 0.321) from the device containing 10% NBu$_4$[EuL$_4$] (Fig. 5: insert) and at 8 V (x = 0.337, y = 0.328) from the device containing 20% NBu$_4$[EuL$_4$] (Fig. 6: insert). This colour change is reversible and thus the emission colour can be tuned by adjusting the voltage. The devices are stable until the device limit is not exceeded, which is at 13 V. However, the devices composed of 30%, 50% and non-doped 100% of NBu$_4$[EuL$_4$] as the emitting layer shows only red emission from the Eu^{III} ion in the entire voltage ranges (Fig. S9-S11 in ESI†).

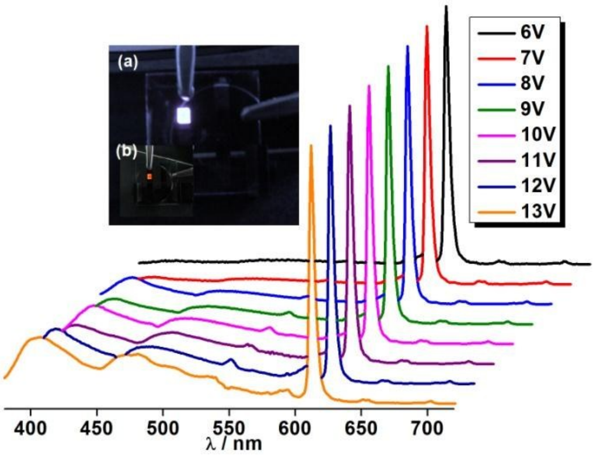

Fig. 6 Electroluminescence spectra of NBu$_4$[EuL$_4$] based on device configuration ITO / PEDOT: PSS (50 nm) / NBu$_4$[EuL$_4$] (20%): CBP (56%)-OXD7 (24%) (50 nm) / TPBI (50 nm) / LiF (1.5 nm) / Al (120 nm) at different bias voltages: inserts photograph of device at 8 V (a) and 7 V (b).

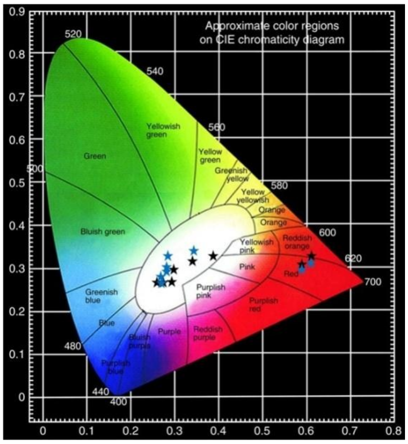

Fig. 7 CIE colour coordinates for devices with 10% (black) and 20% (blue) NBu$_4$[EuL$_4$] at 6–13V.

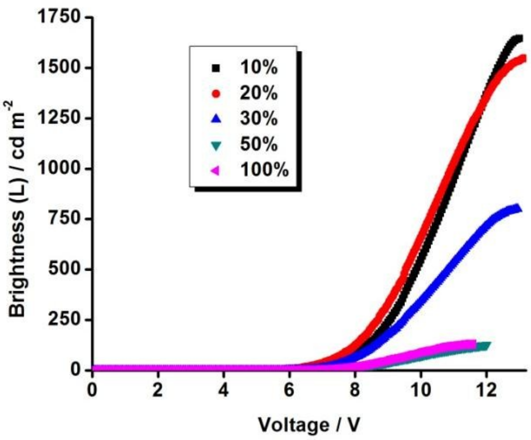

Fig.8 Voltage (*V*) – brightness (*L*) curves of ITO / PEDOT : PSS (50 nm) / NBu$_4$ [EuL$_4$] (10-100%) : CBP:-OXD7 (7 : 3) (50 nm)/ TPBI (50 nm) / LiF (1.5 nm) / Al (120 nm) devices.

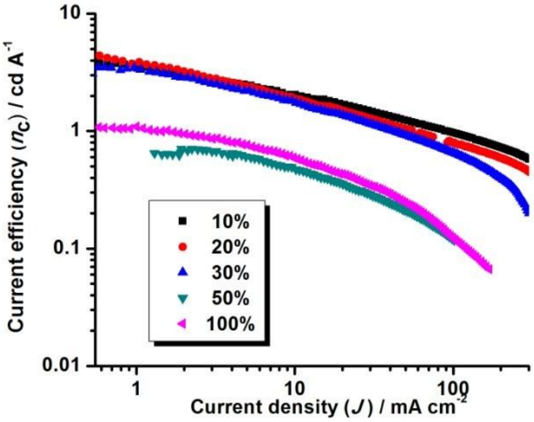

Fig. 9 Current density (*J*) - power efficiency (η_p) curves of ITO / PEDOT: PSS (50 nm) / NBu$_4$[EuL$_4$] (10-100%) : CBP -OXD7 (7 : 3) (50nm) / TPBI (50 nm) / LiF (1.5 nm) / Al (120 nm) devices.

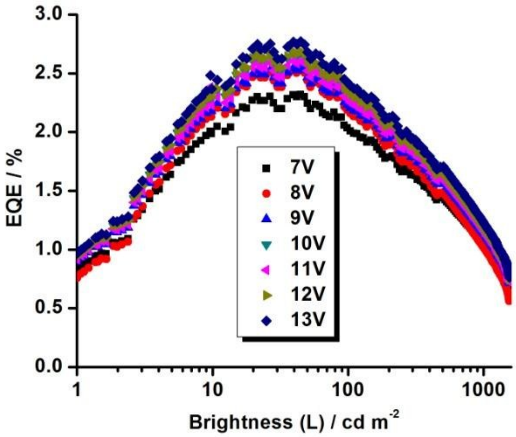

Fig. 10 External quantum efficiency versus brightness of device ITO / PEDOT : PSS (50 nm) / NBu$_4$[EuL$_4$] (20%) : CBP (56%)-OXD7 (24%) (50 nm) / TPBI (50 nm) / LiF (1.5 nm) / Al (120 nm) at 7–13V.

Table 2. EL characteristics of devices containing $NBu_4[EuL_4]$.

doping / %	V_{on} / V	L / cd m^{-2}	η_c / cd A^{-1}	η_p / lm W^{-1}	η_{ext} / %		
					max	L = 100	L = 1000
10	5.25	1645 (13V)	4.39 (7.4 V)	1.89 (7.4 V)	2.6 (13 V)	1.5 (13 V)	0.6 (13 V)
20	4.90	1547 (13 V)	5.14 (6.4V)	2.53 (5.1 V)	2.8 (13 V)	2.4 (13 V)	1.2 (13 V)
30	6.15	801 (13V)	3.56 (7.3 V)	1.54 (7.3 V)	1.9 (12 V)	1.2 (12 V)	—
50	6.55	125 (12 V)	0.91 (8.6 V)	0.33 (8.6 V)	0.4 (10 V)	0.1 (10V)	—
100	6.65	129 (11.6 V)	1.10 (7.3 V)	0.47 (7.3 V)	0.3 (10 V)	0.1 (10 V)	—

Table 3. EL characteristics of WOLEDs containing Eu^{III}-β-diketonates as emitting materials reported in literatures.[a]

Eu^{III}-complex	η_c / cd A^{-1}	η_p / lm W^{-1}	η_{ext} / %	CIE
$NBu_4[EuL_4]$	5.14(6.4V)	2.53 (6.4V)	2.5 (8 V)	0.337, 0.328 (8V)
$Eu(TCPD)_3(Phen)$[27]	—	0.2 (10.5V)	1.1 (10.5V)	0.333, 0.348 (16.2V)
$[(Eu(tta)_3)_2(\mu\text{-bpm})]$[13]	—	—	0.03 (13.3V)	0.350, 0.330 (13.3V)
$Eu(phen)(L1\text{-}Br)(L1)_2$[12]	—	—	0.15	0.320, 0.260
$[Eu(DBM)_3FDPO]_n$[3]	0.71	0.27	0.37	0.380, 0.320

[a] TCPD = 1-[3,4,5-Tris[4-(9H-carbazol-9-yl)butoxy]-phenyl]-3-phenylpropane-1,3-dione, phen = 1,10-Phenanthroline, μ-bpm = 2,2'-Bipyrimidine, L1 = 4, 4, 4-Trifluoro-1-5-(11-(m-toloyloxy)undecyl)thiophen-2-yl)butane-1,3-dione, L1-Br = 1-5-(11-(Bromoundecyl)thiophen-2-yl) 4, 4, 4-trifluorobutane-1,3-dione, tta = 2-Thenoyltrifluoroacetone, DBM = Dibenzoylmethane, FDPO = 9,9-Bis(diphenylphosphorylphenyl)fluorene.

The voltage (V) – brightness (L), current density (J) – current efficiency (η_c), voltage (V) – current density (J) and current density (J) – power efficiency (η_p) curves at various $NBu_4[EuL_4]$ doping concentrations are presented in Figs. 8-9 and Figs. S12-S13 in ESI†. The detailed performances of devices were summarized in Table 2. It can be noticed from Table 2 that the measured parameters of the devices shows slight increase with increasing doping concentration up to 20%, whereas further increase in $NBu_4[EuL_4]$ concentration results in the decrease of device parameters, a possible effect of concentration quenching. The maximum external quantum efficiency (EQE) of 2.8% is obtained for the device with 20wt% doping concentration (Fig. 10) with maximum current efficiency of 5.14 cd A^{-1} and power efficiency of 2.53 lm W^{-1} at 6.4 V. The highest brightness is 1547 cd m^{-2} at 13.1 V. It is well-known that, efficiency of phosphorescent devices decreases significantly with increasing current density due to increased triplet–triplet annihilation at high current density[40] and field-induced quenching effects.[41] However, in the present study, the external quantum efficiency (EQE) of devices showed a moderate drop with increasing current density and brightness (Figs. 10 and S14-S16 in ESI†). In particular, the device with 20% $NBu_4[EuL_4]$ shows EQE of 2.4% at L= 100 cd m^{-2} and 1.2% at 1000 cd m^{-2} (Table S1 in ESI†). To the best of our knowledge, this is the best EL performance of a WOLED based on Eu^{III} complex reported so far in literature (Table 3). Furthermore, the turn-on voltage (V_{on}), which is defined as voltage at 1 cd m^{-2} and voltage required to obtain white light (V_{white}) shown by the devices in the present study are 4.9–6.7 V and 8 V, respectively. These values are considerably lower than those obtained for the device having Eu^{III}-complex with carbazole substituted dendritic ligand, (V_{on} = 10.5 and V_{white} = 16V).[27]

Conclusions

A novel luminescent Eu^{III} tetrakis-β-diketonate complex containing carbazole unit has been synthesized and characterized. The EL devices fabricated from the new complex doped into CBP : OXD7 mixed host as the emitting layer show good performance. Devices with 10% and 20% of $NBu_4[EuL_4]$ shows white-light emission with maximum EQE of 2.6% and 2.8%, the highest EQE reported so far for WOLEDs based on Eu^{III} complexes. Due to the presence of carbazol-9-yl-biphenyl group in the ligand, a significant reduction of turn-on voltage and improvement of device efficiency was noticed, because of probably good energy level matches and phase compatibility for $NBu_4[EuL_4]$ with the host. Furthermore, the strong electron affinity of $NBu_4[EuL_4]$ contributes to improve electron injection into the emitting layer and causes balanced charge injection and transport, which accounts for the red EL emission from a host free device ITO / PEDOT : PSS (50 nm) / $NBu_4[EuL_4]$ (50 nm) / TPBI (50 nm) / LiF (1.5 nm) / Al (120 nm). Currently, research is progressing in our laboratory on the development of stable Ln^{III}-complexes containing phosphine oxides and N-donor ligands with the aim of further improving the EL properties. Preliminary results are encouraging.

Acknowledgements

This research was supported by the NSFC (91122006, 21390392, 21473201 and U1405252), the 973 project (2014CB845603) from

MSTC, and the CAS/SAFEA International Partnership Program for Creative Research Teams. The authors thank Prof. Jef Rozenski, The Association of Biomolecular Recourse Facilities, Rega Institute KU Leuven for HRMS analysis. One of the authors (S. B.) thanks Collegiate Education Dept. and Dept. of Higher Education Govt. of Kerala, India for granting leave without allowance for doing post-doctoral research.

Notes and references

State Key Laboratory of Structural Chemistry, Fujian Institute of Research on the Structure of Matter, Chinese Academy of Science, Fuzhou, Fujian 35002, People's Republic of China
Email: czn@fjirsm.ac.cn

† Electronic Supplementary Information (ESI) available: NMR, TGA, CV and EL data. See DOI: 10.1039/b000000x/

1 G. M. Farinola and R. Ragni, *Chem. Soc. Rev.*, 2011, **40**, 3467.
2 M. A. Katkova and M. N. Bochkarev, *Dalton Trans.*, 2010, **39**, 6599.
3 H. Xu, J. Wang, Y. Wei, G. Xie, Q. Xue, Z. Deng and W. Huang, *J. Mater. Chem. C,* 2015, **3**, 1893.
4 Eliseeva, S. V. Bünzli, J.-C. G. *Chem. Soc. Rev.*, 2010, **39**, 189.
5 J. Kido, W. Ikeda, M. Kimura and K. Nagai, *Jpn. J. Appl. Phys.*, 1996, **35**, L394.
6 D. Zhao, W. Li, Z. Hong, X. Liu, C. Liang and D. Zhao, *J. Lumin.*, 1999, **82,** 105.
7 W. G. Quirino, C. Legnani, M. Cremona, P. P. Lima, S. Alves Jr. and O. L. Malta. *Thin Solid Films*, 2006, **494**, 23.
8 J. Mezyk, W. Mroz, A. Mech, U. Giovanella, F. Meinardi, C. Botta, B. Vercelli and R. Tubino, *Phys. Chem. Chem. Phys.*, 2009, **11**, 10152.
9 G. He, D. Guo, C. He, X. Zhang, X. Zhao and C. Duan, *Angew. Chem.*, 2009, **121**, 6248.
10 J. Liu, Y. Cheng, Z. Xie, Y. Geng, L. Wang, X. Jing and F. Wang, *Adv. Mater.*, 2008, **20**, 1357.
11 J. Liu, Z. Y. Xie, Y. X. Cheng, Y. H. Geng, L. X. Wang, X. B. Jing and F. S. Wang, *Adv. Mater.*, 2007, **19**, 531.
12 U. Giovanella, M. Pasini, C. Freund, C. Botta, W. Porzio and S. Destri, *J. Phys. Chem. C*, 2009, **113**, 2290.
13 G. Zucchi, T. Jeon, D. Tondelier, D. Aldakov, P. Thuery, M. Ephritikhine and B. Geffroy, *J. Mater. Chem.*, 2010, **20**, 2114.
14 G. -L. Law, K. -L. Wong, H. -L. Tam, K. -W. Cheah and W. -T. Wong, *Inorg. Chem.*, 2009, **48**, 10492.
15 S. Biju, M. L. P. Reddy, A. H. Cowley and K. V. Vasudevan, *J. Mater. Chem.*, 2009, **19**, 5179.
16 O. L. Malta, H. F.Brito, J. F. S. Menezes, F. R. G. Silva, S. Alves Jr, F. S. Farias Jr and A. V.M. de Andrade, *J. Lumin.*, 1997, **75**, 255.
17 D. B. A. Raj, B. Francis, M. L. P. Reddy, R. R. Butorac, V. M. Lynch and A. H. Cowley, *Inorg. Chem.*, 2010, **49**, 9055.
18 K. Binnemans, *Chem. Rev.*, 2009, **109**, 4283.
19 J. Feng, and H. Zhang, *Chem. Soc. Rev.*, 2013, **42**, 387.
20 J. Kido, Y. Okamoto, *Chem. Rev.*, 2002, **102**, 2357.
21 J. V. Grazulevicius, P. Strohriegl, J. Pelichowski and K. Pelichowski, *Prog. Polym. Sci.*. 2003, **28**, 1297.
22 J. Li and A. C. Grimsdale, *Chem. Soc. Rev*., 2010, **39**, 2399.
23 D. Nie, Z. Chen, Z. Bian, J. Zhou, Z. Liu, F. Chen, Y. Zhao and C. Huang, *New J. Chem.*, 2007, **31**, 1639.
24 M. R. Robinson, M. B. O'Regan, and G. C. Bazan, *Chem. Commun.*, 2000, 1645.
25 J. -F. Morin, M. Leclerc, D. Adès and A. Siove, *Macromol. Rapid Commun.*, 2005, **26**, 761.
26) P. He, H. H. Wang, S. G. Liu, J. X. Shi, G. Wang and M. L. Gong, *Inorg. Chem.*, 2009, **48**, 11382.
27 S. Li, G. Zhong, W. Zhu, F. Li, J. Pan, W. Huang and H. Tian, *J. Mater. Chem.*, 2005, **15**, 3221.
28 Q. Ma, Y. Zheng, N. Armaroli, M. Bolognesi and G. Accorsi, *Inorg. Chim. Acta.*, 2009, **362**, 3181.
29 S. Biju, Y. K. Eom, J. C. -G. Bünzli and H. K. Kim, *J. Mater. Chem. C*, 2013, **1**, 6935.
30 S. Biju, R. O. Freire, Y. K. Eom, R. Scopelliti, J. -C. G. Bünzli and H. K. Kim, *Inorg. Chem.*, 2014, **53**, 8407.
31 G. A. Crosby, R. E. Whan, and R. M. Alire, *J. Chem. Phys.*, 1961, **34**, 743.
32 S. Comby and J.-C. G.Bünzli, In *Handbook on the Physics and Chemistry of Rare Earths*; Karl A. Gschneidner, J.-C. G.Bünzli, V. K. Pecharsky, Ed.; Elsevier, 2007; Vol. Volume 37; pp 217.
33 S. Biju, D. B. A. Raj, M. L. P. Reddy and B. M. Kariuki, *Inorg. Chem.*, 2006, **45**, 10651.
34 Biju, S. M. L. P. Reddy, A. H. Cowley and K. V. Vasudevan, *Cryst. Growth Des.*, 2009, **9**, 3562.
35 V. Divya, S. Biju, R. L. Varma, and M. L. P. Reddy, *J. Mater. Chem.*, 2010, **20**, 5220.
36 D. B. A. Raj, S. Biju and M. L. P. Reddy, *Inorg. Chem.* 2008, **47**, 8091.
37 M.-H. Ha-Thi, J. A. Delaire, V. Michelet and I. Leray, *J. Phys. Chem. A* 2009, **114**, 3264.
38 S. Biju, Y. K. Eom, J. C. -G. Bünzli and H. K. Kim *J. Mater. Chem. C*, 2013, **1**, 3454.
39 V. Adamovich, J. Brooks, A. Tamayo, A. M. Alexander, P. I. Djurovich, W. B. D'Andrade, C. Adachi, S. R. Forrest and M. E. Thompson, *New J. Chem.*, 2002, **26**, 1171.
40 C. Adachi, M. A. Baldo and S. R. Forrest, *J. Appl. Phys.*, 2000, **87**, 8049.
41 J. Kalinowski, W. Stampor, J. Mężyk, M. Cocchi, D. Virgili, V.Fattori and P. Di Marco, *Phys. Rev. B: Condens. Matter*., 2002, **66**, 235321.

TOC for

White OLEDs Based on a Novel Eu^{III}–Tetrakis–β–Diketonate Doped into 4,4'-*N,N'*-Dicarbazolebiphenyl as Emitting Material†

Silvanose Biju, Liang-Jin Xu, Cheng-Zhe Sun and Zhong-Ning Chen

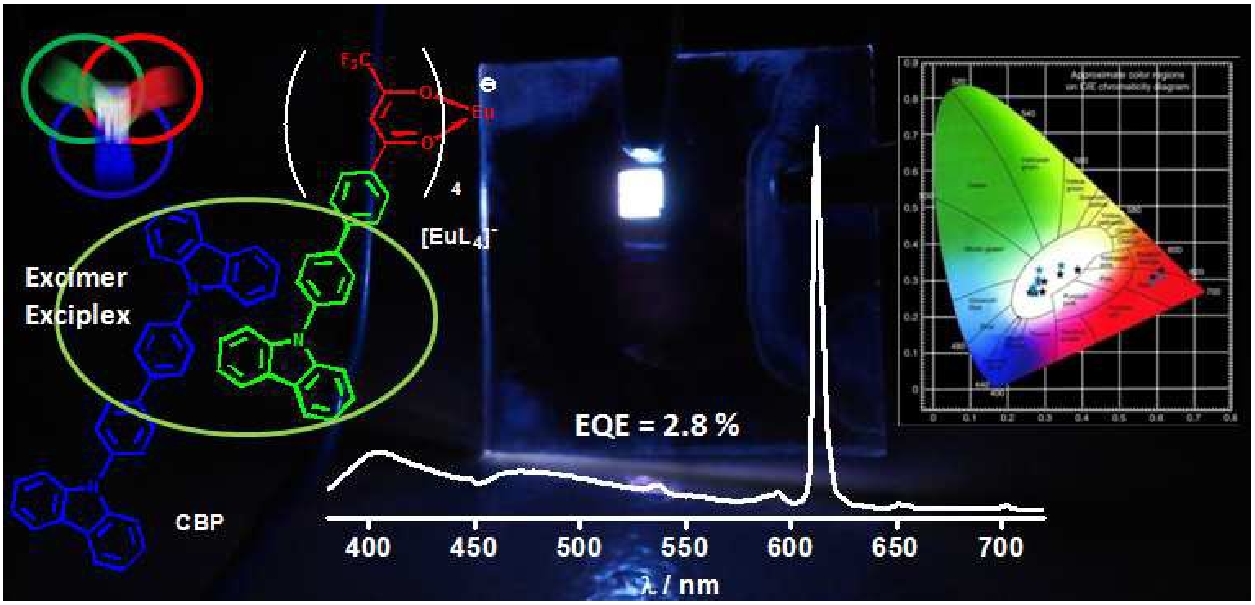

White OLED's with external quantum efficiency (EQE) 2.8%, maximum brightness (L) of 1547 cd m^{-2}, current efficiency (η_c) of 5.14 cd A^{-1} and power efficiency (η_p) of 2.53 lmW^{-1} were fabricated using a newly developed Eu^{III}–tetrakis–β–diketonate compound.